AD-A219 128

Technical Report 1329
November 1989

Contributions of Individual Structural Modes to the Scattered Acoustic Field

G. W. Benthien

NAVAL OCEAN SYSTEMS CENTER
San Diego, California 92152-5000

J. D. FONTANA, CAPT, USN
Commander

R. M. HILLYER
Technical Director

ADMINISTRATIVE INFORMATION

This work was performed by the Transduction Sciences Branch, Code 712, Naval Ocean Systems Center, for the Naval Research Laboratory as part of the Target Physics Block Program sponsored by the Office of Naval Technology.

Released by
C. L. Meland, Head
Transduction Sciences Branch

Under authority of
T. F. Ball, Head
Acoustic Systems and
Technology Division

ACKNOWLEDGMENTS

The author would like to thank Don Barach and David Gillette for converting the techniques described in this report into efficient computer programs and for obtaining the included numerical results. The author would also like to thank H. A. Schenck for his review of this paper and for many useful discussions and suggestions.

JG

SUMMARY

The frequency behavior of the scattered acoustic field produced by a plane wave impinging on an elastic body immersed in an infinite fluid medium is dominated in certain frequency ranges by large peaks arising from resonant modes in the elastic structure. Computational models have been developed at the Naval Ocean Systems Center for solving these elastic scattering problems. This report shows that the scattered pressure can be represented as a sum of contributions from *in vacuo* modes of the structure. The spectral response of individual terms in this summation can be used to identify which modes contribute to each peak in the overall spectral response of the scattered field. In many cases a small number of modes dominate the response in the vicinity of these peaks.

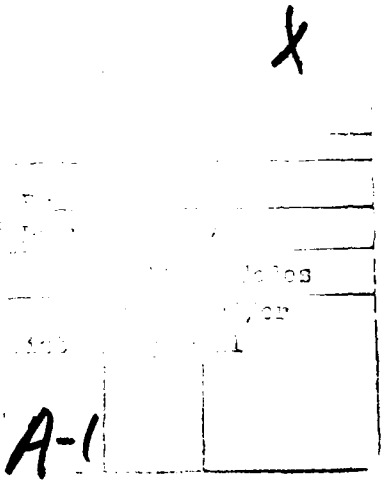

CONTENTS

FIGURES

TABLE

INTRODUCTION

The frequency behavior of the scattered acoustic field produced by a plane wave impinging on an elastic body immersed in an infinite fluid medium is dominated in certain frequency ranges by large peaks arising from resonant modes in the elastic structure. A technique for computing the scattered acoustic field was described in a previous Naval Ocean Systems Center (NOSC) technical report (Schenck and Benthien, 1989). This technique makes use of a finite element model of the elastic structure and a Helmholtz integral model (CHIEF) (Benthien, Barach, and Gillette, 1988) (Schenck, 1968) of the acoustic medium. The purpose of the present report is to show how quantities computed with the above technique can be used to identify which *in vacuo* structural modes are the main contributors to each peak in the scattered field frequency response.

The second section of this report contains a brief survey of the numerical approach used to solve the acoustic scattering problem as well as the basic equations needed for identifying modal contributions. The third section contains numerical results obtained by applying the modal identification technique to two scattering problems. The fourth section contains a brief summary of conclusions which illustrate the utility of this technique in understanding the underlying structure of the scattered field.

BASIC EQUATIONS

Throughout this section all pressures, displacements, and velocities will be represented by their complex, frequency dependent Fourier components corresponding to the time dependence $e^{i\omega t}$. The elastic structure is modeled using the finite element equations (Zienkiewicz, 1977)

$$(-\omega^2 M + K)U = F, \tag{1}$$

where M is the mass matrix, K is the stiffness matrix, F is the load vector, and U is a vector whose components are the displacement degrees-of-freedom at all the nodes in the body. In the scattering problem under investigation, the load vector F is completely determined by the acoustic pressure p on the wet surface S of the body. The components of F are given by

$$F_m = -\int_S p\,\boldsymbol{\phi}_m \cdot \boldsymbol{n}\, dS, \tag{2}$$

where p is the acoustic pressure, $\boldsymbol{n}$ is a unit normal to S pointing into the fluid, and $\boldsymbol{\phi}_m$ is a finite element vector interpolation function. The displacement $\boldsymbol{u}(x)$ at a point x in the body can be expressed in terms of the interpolation functions $\boldsymbol{\phi}_m$ as follows:

$$\boldsymbol{u}(x) = \sum_{m=1}^{M} U_m \boldsymbol{\phi}_m(x), \tag{3}$$

where $U_1, \ldots, U_M$ are the components of U.

The CHIEF formulation of the acoustic part of the problem is based on the Helmholtz integral relations. The surface Helmholtz integral equation is approximated by the system of algebraic equations

$$AP = BV + P^{inc}, \tag{4}$$

where the matrices A and B involve integrals of the free-space Green's function and its normal derivative over the subdivisions S_n of S; P and V are vectors whose nth components are the pressure and normal velocity (assumed to be constant) on the subdivision S_n of S; and P^{inc} is a vector (Benthien, et al., 1988) whose nth component is the value of the incident pressure wave at a reference point on S_n. The scattered pressure p^s at a field point x exterior to the body can be approximated by

$$p^s(x) = a^T(x)P + b^T(x)V, \tag{5}$$

where $a(x)$ and $b(x)$ are vectors whose components (Benthien, et al., 1988) involve integrals of the free-space Green's function and its normal derivative over the subdivisions S_n and evaluated at the field point x. Equations (4) and (5) can be combined to give

$$p^s(x) = q^T(x)V + p^{rs}(x), \tag{6}$$

where

$$q^T(x) = a^T(x)A^{-1}B + b^T(x)$$

and

$$p^{rs}(x) = a^T(x)A^{-1}P^{inc}.$$

It can be seen from equation (6) that $p^{rs}(x)$ is the rigid scattering from the body (i.e., the scattered pressure when v is constrained to be zero).

Applying the assumption that p is piecewise constant on the subdivisions of S to equation (2), gives

$$F = -CDP, \tag{7}$$

where

$$C_{mn} = \frac{1}{S_n}\int_{S_n} \boldsymbol{\phi}_m \cdot \boldsymbol{n}\, dS$$

and

$$D = \mathrm{diag}(S_1, S_2, \ldots, S_N).$$

Equations (1) and (7) can be combined to give

$$U = -(-\omega^2 M + K)^{-1}CDP. \tag{8}$$

Since different interpolation schemes are used in the finite element model of the structure and the CHIEF model of the acoustic medium, it is impossible to enforce exact continuity of normal displacement across S. However, this continuity is approximately enforced by equating the CHIEF normal velocity v_n to the average of the finite-element normal velocity over S_n, i.e.,

$$v_n = \frac{1}{S_n}\int_{S_n} i\omega \boldsymbol{u} \cdot \boldsymbol{n}\, dS. \tag{9}$$

Combination of equations (3), (8), and (9) gives

$$\begin{aligned} V &= i\omega C^T U \\ &= -i\omega C^T(-\omega^2 M + K)^{-1}CDP. \end{aligned} \tag{10}$$

Let E be a matrix whose columns are the *in vacuo* normal modes of the structure, i.e.,

$$KE = ME\Omega, \tag{11}$$

where $\Omega = \mathrm{diag}(\omega_1^2, \ldots, \omega_M^2)$ is the diagonal matrix of eigenfrequencies. Since the modes are M-orthogonal, they can be normalized so that

$$E^T M E = I. \tag{12}$$

It is easily verified that the inverse matrix $(-\omega^2 M + K)^{-1}$ can be expressed in terms of the normal mode matrix E as follows:

$$(-\omega^2 M + K)^{-1} = E(-\omega^2 I + \Omega)^{-1} E^T. \tag{13}$$

This form is convenient since the diagonal matrix $(-\omega^2 I + \Omega)$ is easily inverted at all frequencies. Combination of equations (10) and (13) gives

$$V = -i\omega C^T E(-\omega^2 I + \Omega)^{-1} E^T C D P. \tag{14}$$

Equations (4) and (14) can now be combined to give

$$[A + i\omega B C^T E(-\omega^2 I + \Omega)^{-1} E^T C D]P = P^{inc}. \tag{15}$$

Equation (15) can be solved for the surface pressure vector P. Once P is determined, the velocity vector V can be obtained from equation (14) and the scattered pressure $p^s(x)$ can be computed at any exterior field point x using equations (5) or (6).

The remainder of this section will be devoted to the development of a modal expansion for $p^s(x)$. Each column of E represents an *in vacuo* mode of the structure. If e_n is the nth column of E, then equation (13) can be written in the alternate form

$$(-\omega^2 M + K)^{-1} = \sum_{m=1}^{M} \frac{1}{\omega_m^2 - \omega^2} e_m e_m^T. \tag{16}$$

Combination of equations (8) and (16) gives

$$U = \sum_{m=1}^{M} \left(\frac{e_m^T C D P}{\omega^2 - \omega_m^2} \right) e_m. \tag{17}$$

In view of equation (10), it follows that

$$V = i\omega \sum_{m=1}^{M} \left(\frac{e_m^T C D P}{\omega^2 - \omega_m^2} \right) C^T e_m. \tag{18}$$

Substitution of equation (18) into equation (6) gives

$$p^s(x) - p^{rs}(x) = i\omega \sum_{m=1}^{M} \left(\frac{e_m^T C D P}{\omega^2 - \omega_m^2} \right) q^T(x) C^T e_m. \tag{19}$$

The nth term of the sum in equation (19) is the contribution of the mode e_n to the scattered field. Once equation (15) is solved for P, the contributions of various modes can be determined by plotting individual terms of equation (19) or partial sums of equation (19) versus frequency and comparing the results with the plots of $p^s(x) - p^{rs}(x)$ versus frequency.

NUMERICAL RESULTS

In this section, the results of the previous section will be applied to two scattering problems. The first problem consists of determining the scattered acoustic field produced when a plane incident wave strikes a hollow spherical shell. The ratio of the shell thickness to the mean radius is 0.03 . The material parameters of the shell are

- Density = 7669 Kg/m^3
- Young's modulus = 2.07×10^{11}
- Poisson's ratio = 0.3 .

The material properties of the water are

- Density = 998 Kg/m^3
- Sound Speed = 1486 m/s.

Figure 1 shows the contributions of the second (the so-called accordion) mode to the magnitude of the form function. The dotted curve is the sum of the rigid scattering form function and the form function obtained by using the $m = 2$ term of equation (19). It should be noted that the eigenfrequency of mode 2 *in vacuo* occurs at a ka of 2.55, whereas its contribution to the overall response occurs at a ka of about 1.58 due to the mass-like loading of the acoustic field. Figure 2 shows a similar result for the fourth structural mode. In fact, each of the peaks shown in the overall response is primarily due to a single (higher frequency) *in vacuo* mode of the spherical shell. This simple situation is not usually observed in the scattered field produced by other shapes where peaks are often due to the interaction of several structural modes. This will be illustrated in the second example.

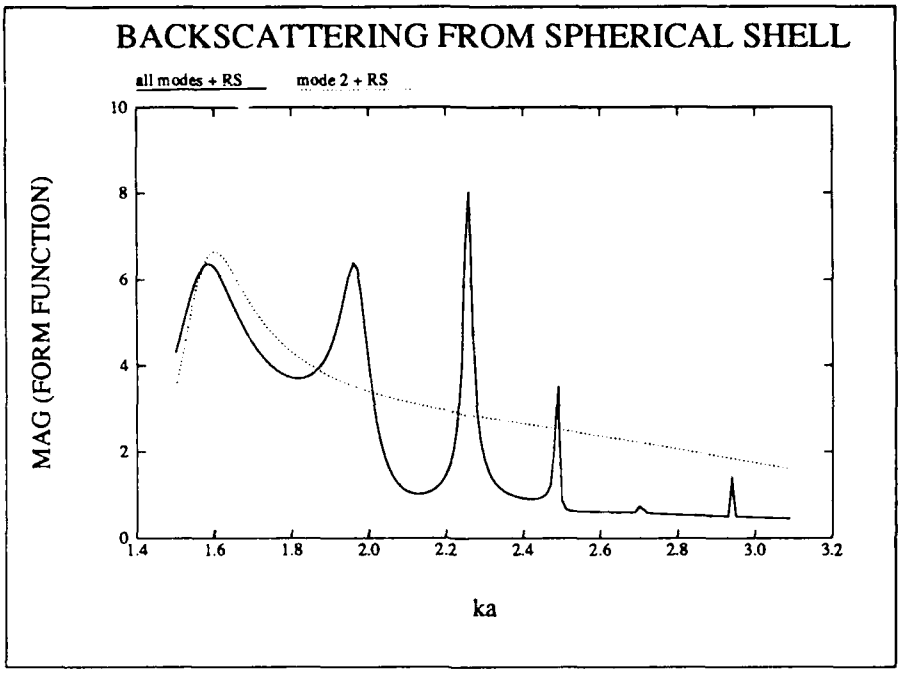

Figure 1. Contribution of mode 2 to backscattering from spherical shell.

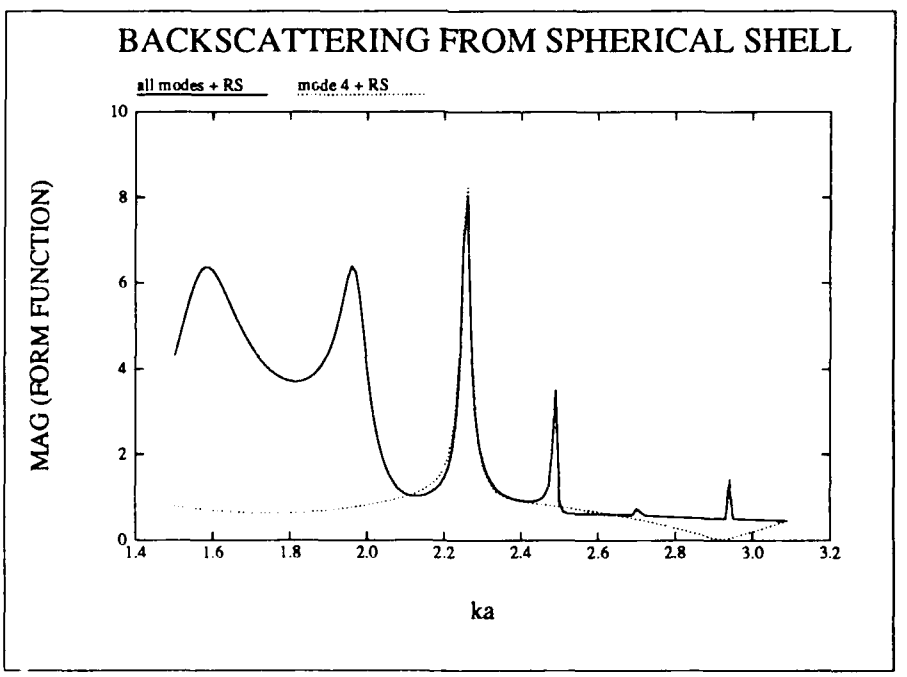

Figure 2. Contribution of mode 4 to backscattering from spherical shell.

The second example involves the backscattering off the end of a capped cylindrical shell. The ratio of the mean radius a to the length L of the shell is 0.125, and the ratio of the thickness h to the mean radius a of the shell is 0.01016 . The ends of the cylinder are capped with circular disks having the same thickness as the shell. The material properties of both the shell and endcaps are

- Density = 8977 Kg/m^3
- Young's modulus = 2.09×10^{11} N/m^2
- Poisson's ratio = 0.308 .

The material properties of the water are

- Density = 998 Kg/m^3
- Sound Speed = 1486 m/s.

The dotted curves in figures 3 to 8 represent the contribution of selected individual terms in the summation shown in equation (19) to the backscattering off the end of the cylinder. The scattered pressure is normalized by the high-frequency plane-wave approximation to the rigid backscattered pressure. The plane wave approximation involves setting $p_s = \rho c v_s$ on the surface, where p_s and v_s are the scattered pressure and normal velocity respectively. For a rigid body, the scattered and incident normal velocities on the surface are related by $v_s = -v_{inc}$. Thus, the plane wave approximation reduces to setting $p_s = -\rho c v_{inc}$ on the surface. The far-field scattered pressure can be obtained from the approximate values of p_s and v_s on the surface. The normalized scattered pressure used in this report is very similar to the form function, which is defined to be the ratio of the scattered pressure to the geometric acoustics approximation of the scattered pressure. In fact, for a sphere, the two normalizations are the same. The normalized frequency ka is defined by $ka = 2\pi f a/c$ where f is the frequency, a is the mean radius, and c is the sound speed in water. The dotted curves in figures 9 and 10 represent the contribution of a partial sum of selected terms in equation (19) to the scattered field. The solid curve in each of these figures represents the normalized pressure (in dB) with the rigid scattering excluded. Figures 11 to 16 show the *in vacuo* mode shapes of the modes used in figures 3 to 8. It is clear from these figures that certain of the peaks in the scattered field are due to a single *in vacuo* mode. For example, the first peak at about $ka = 0.045$ is primarily due to mode 2 (see figure 3). As can be seen from figure 11, mode 2 is predominately an end cap mode. However, certain features such as the hump in the $ka = 0.3$–0.5 range and the humps in the $ka = 0.6$– 1.0 range require the contribution of several *in*

vacuo modes (see figures 9 and 10). Figures 17 and 18 show the surface pressure and normal velocity on the cylinder at $ka = 0.04228$. Notice that the normal velocity distribution is very similar to the *in vacuo* mode shape 2. Figures 19 and 20 show the surface pressure and normal velocity on the cylinder at $ka = 0.95136$. Since multiple modes are involved at this frequency, there is no correspondence between the normal velocity distribution and any single mode shape.

Since the total number of *in vacuo* modes used is often very large, it is useful to first scan a frequency range to determine which modal contributions exceed a preset threshold. The results of a sample scan are shown in table 1 for the cylinder problem, with a threshold of 10 dB over the frequency range $ka = 0.025$–0.3 .

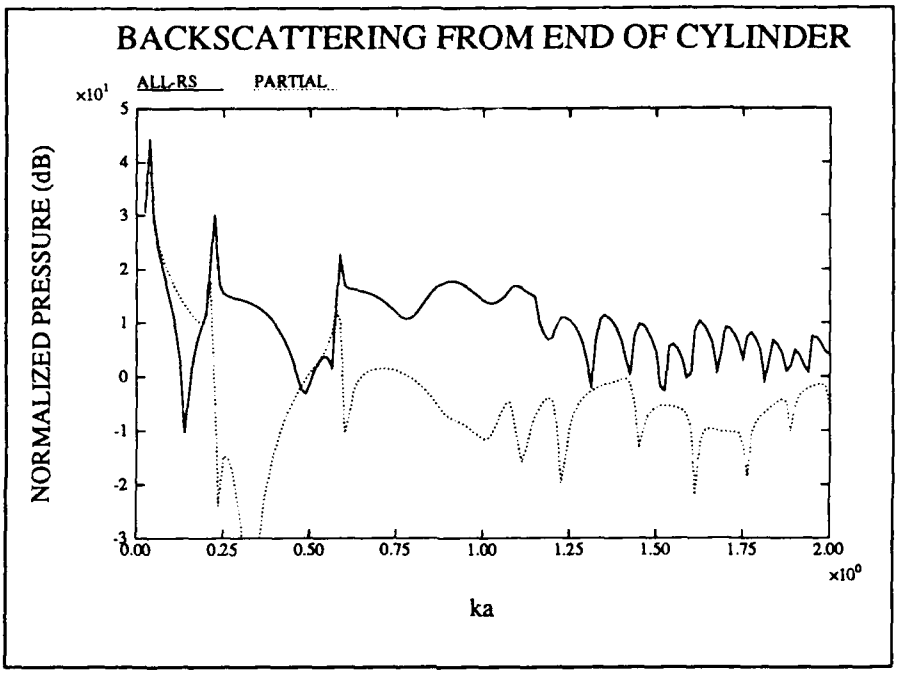

Figure 3. Contribution of mode 2 to scattering from cylinder.

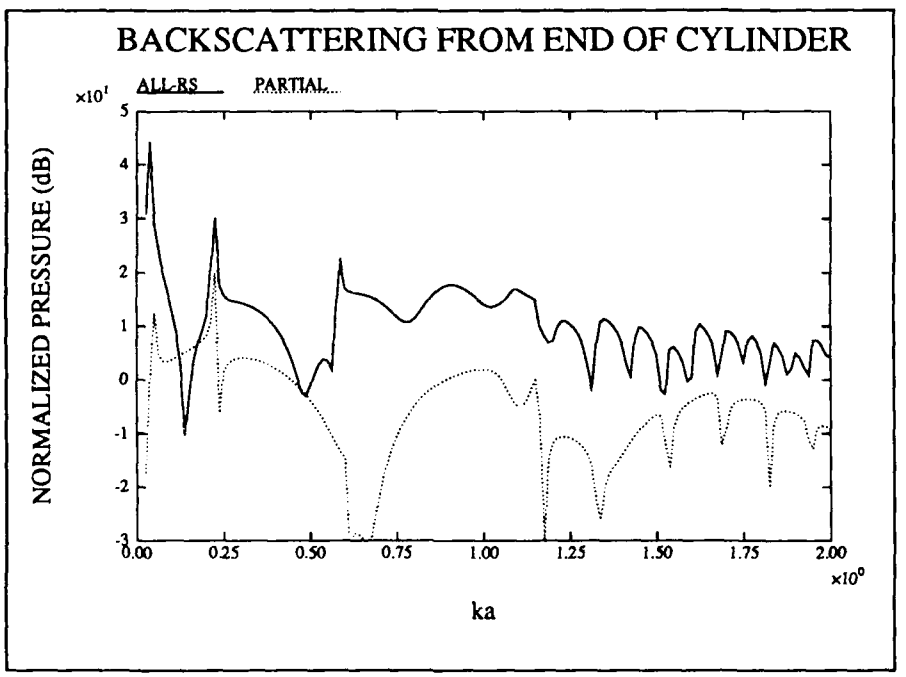

Figure 4. Contribution of mode 3 to scattering from cylinder.

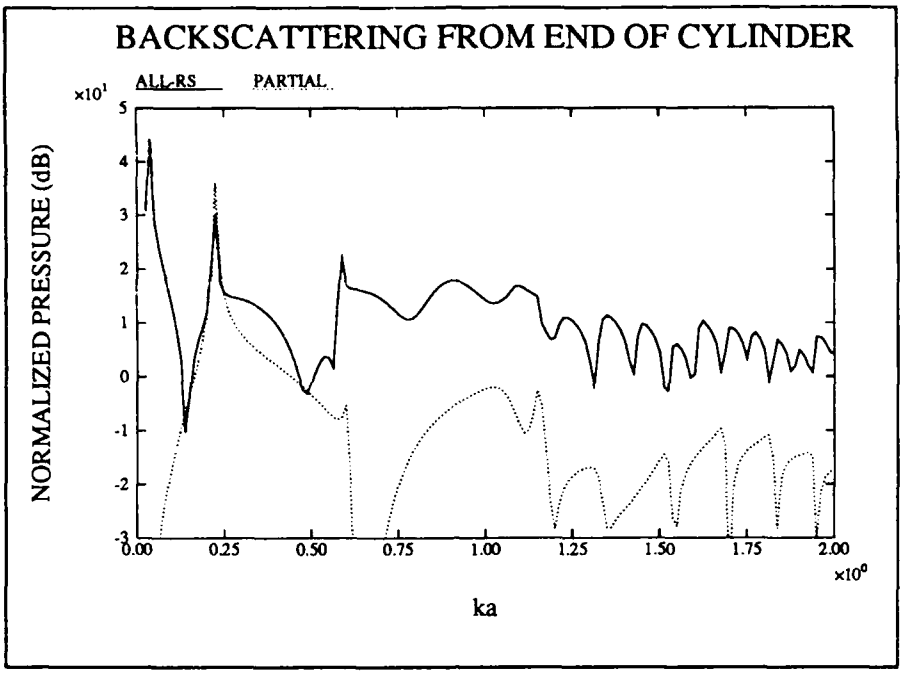

Figure 5. Contribution of mode 5 to scattering from cylinder.

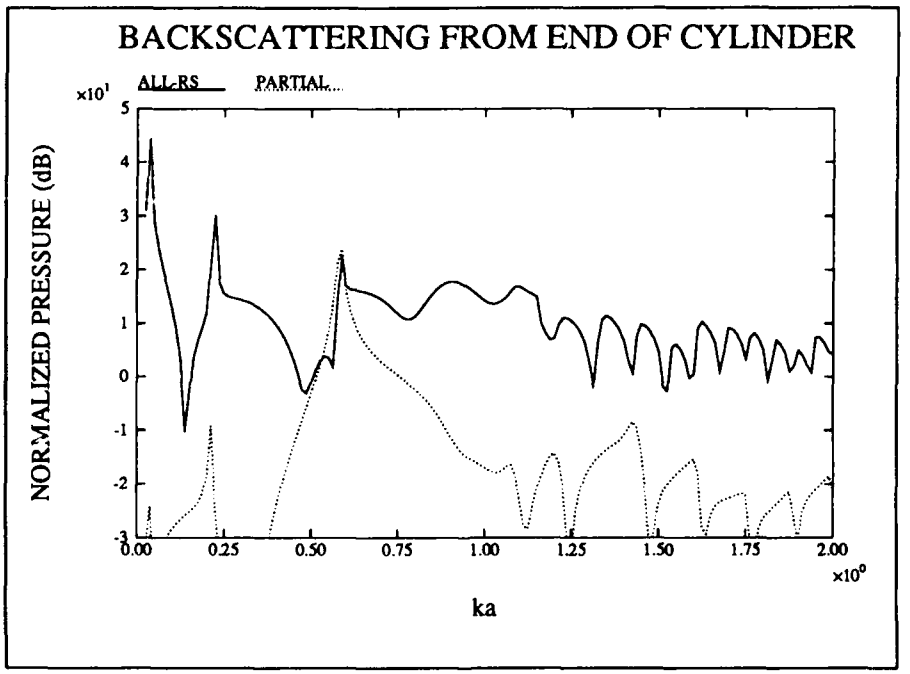

Figure 6. Contribution of mode 6 to scattering from cylinder.

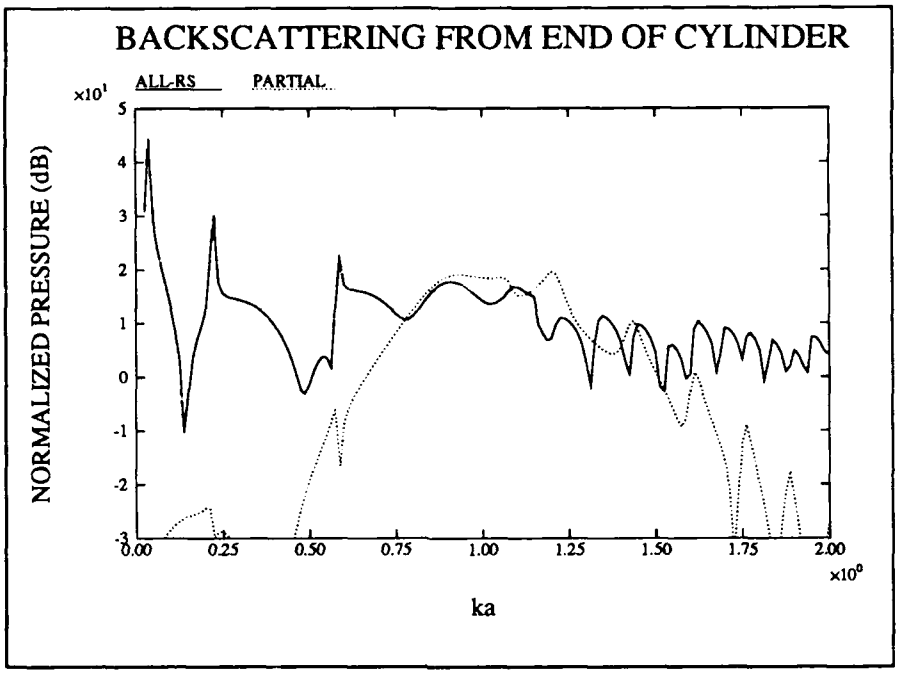

Figure 7. Contribution of mode 14 to scattering from cylinder.

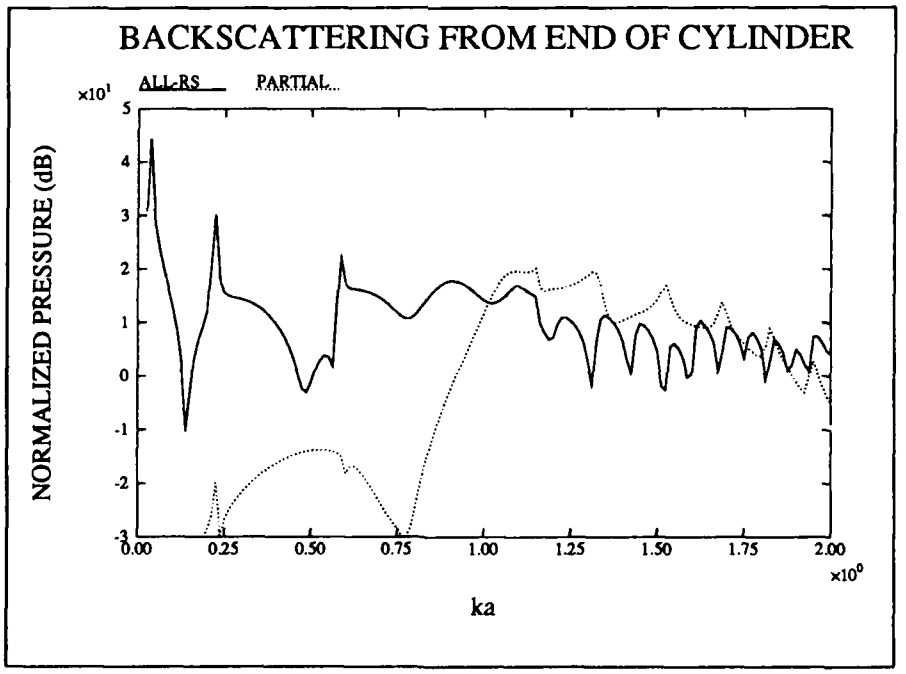

Figure 8. Contribution of mode 15 to scattering from cylinder.

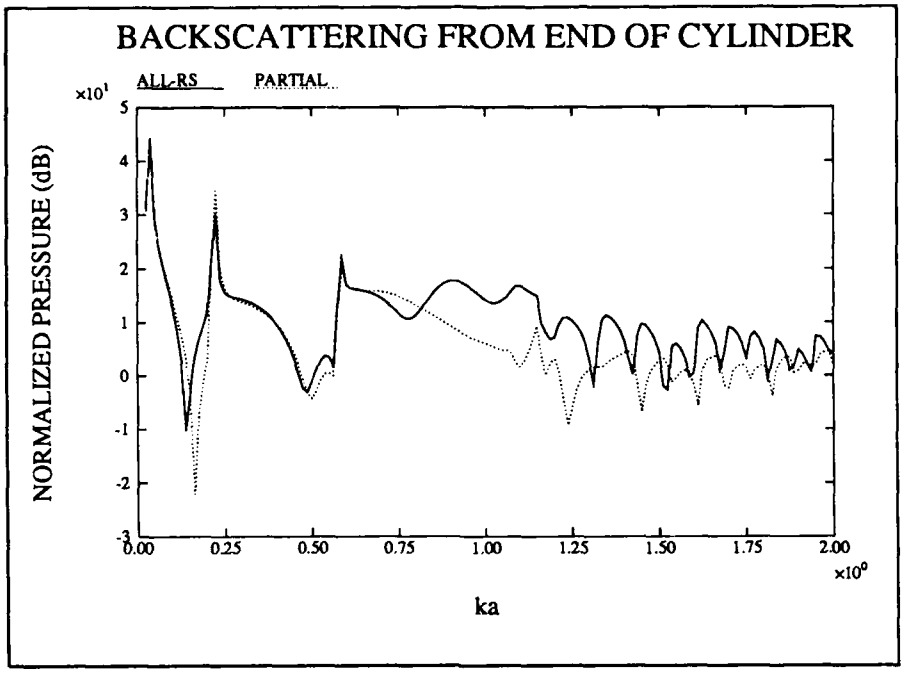

Figure 9. Contribution of modes 2,3,4,5,6,38,44.

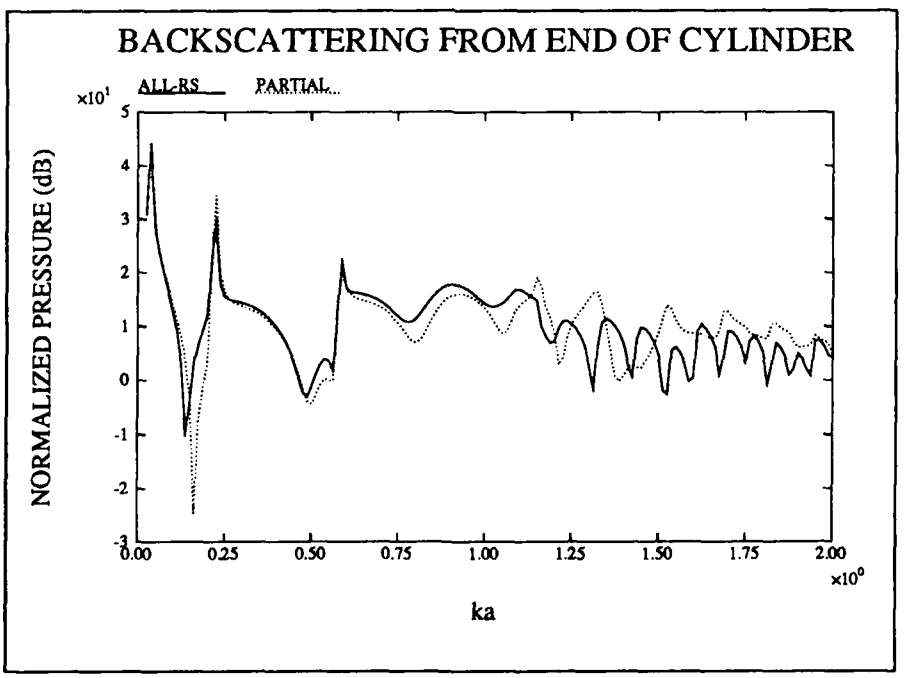

Figure 10. Contribution of modes 2,3,4,5,6,14,15,38,44.

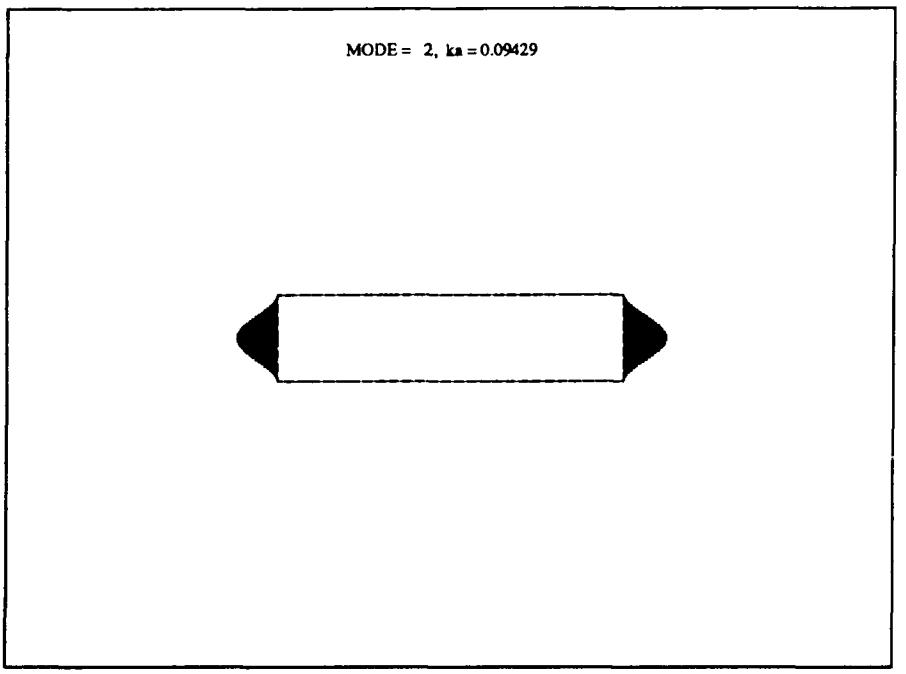

Figure 11. Cylinder mode shape 2.

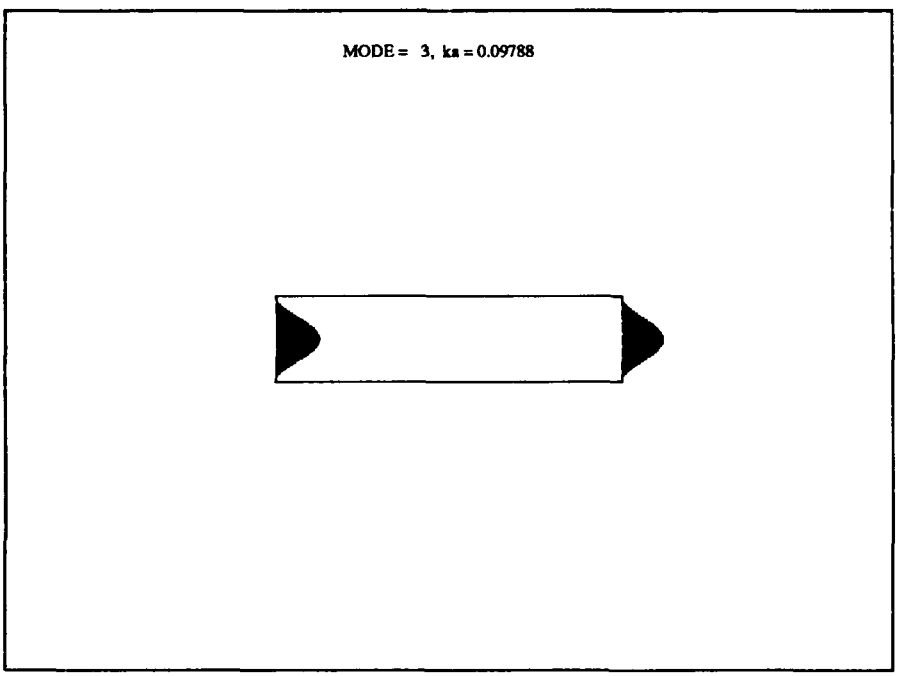

Figure 12. Cylinder mode shape 3.

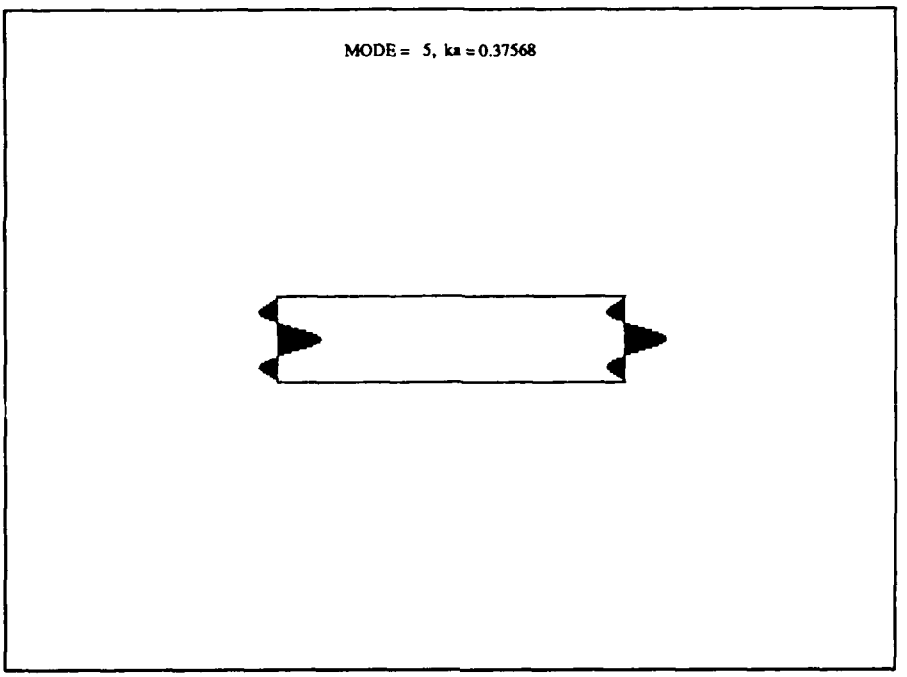

Figure 13. Cylinder mode shape 5.

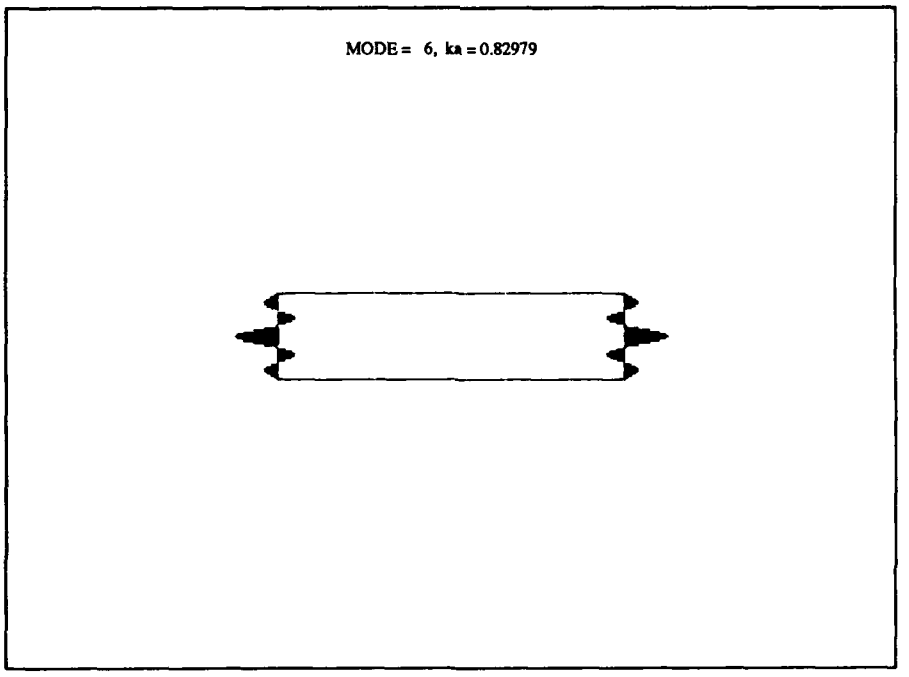

Figure 14. Cylinder mode shape 6.

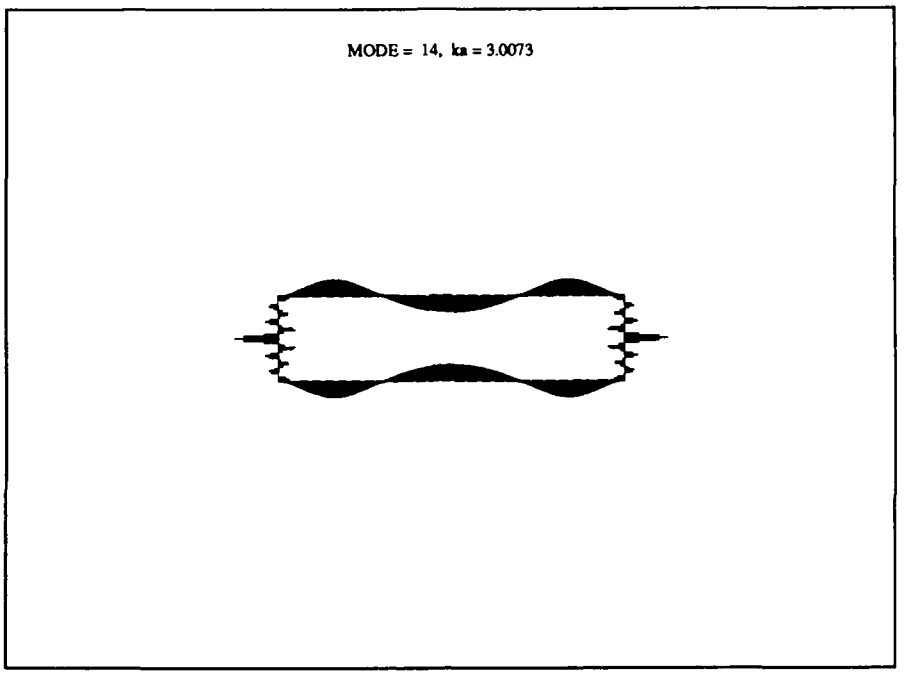

Figure 15. Cylinder mode shape 14.

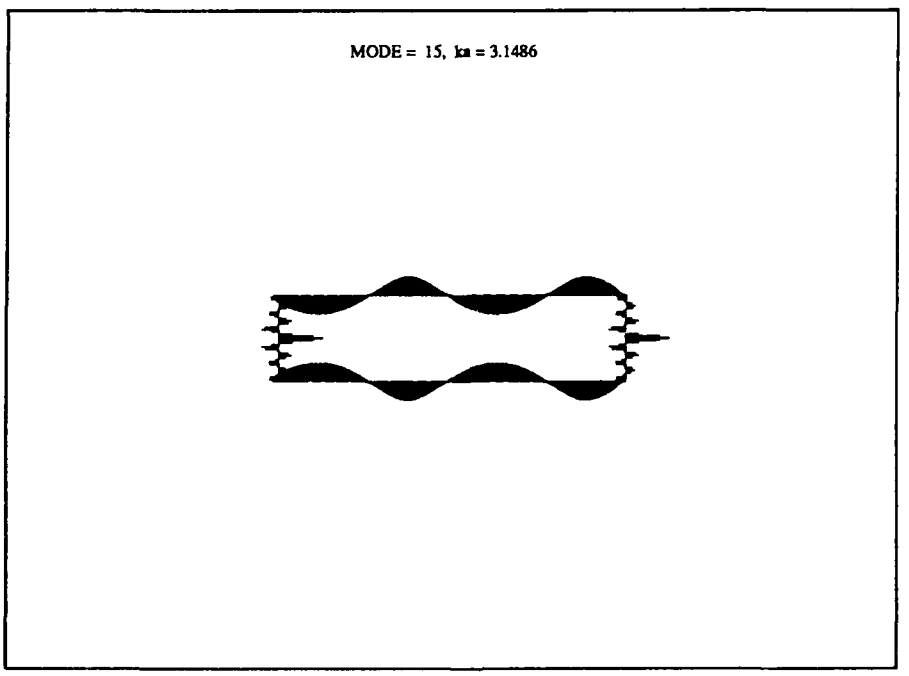

Figure 16. Cylinder mode shape 15.

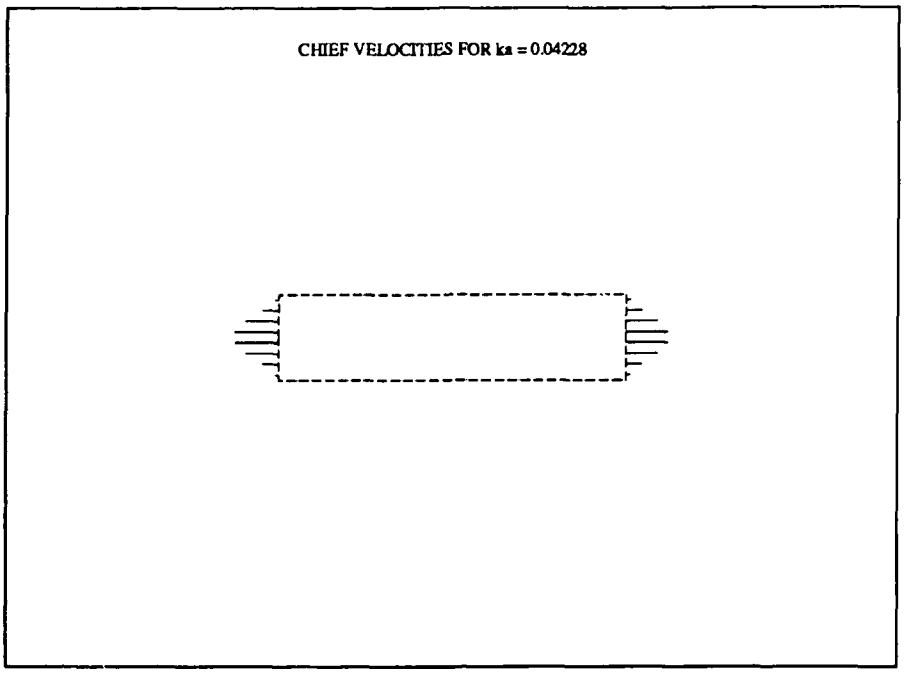

Figure 17. Normal velocity on cylinder, ka = 0.04228.

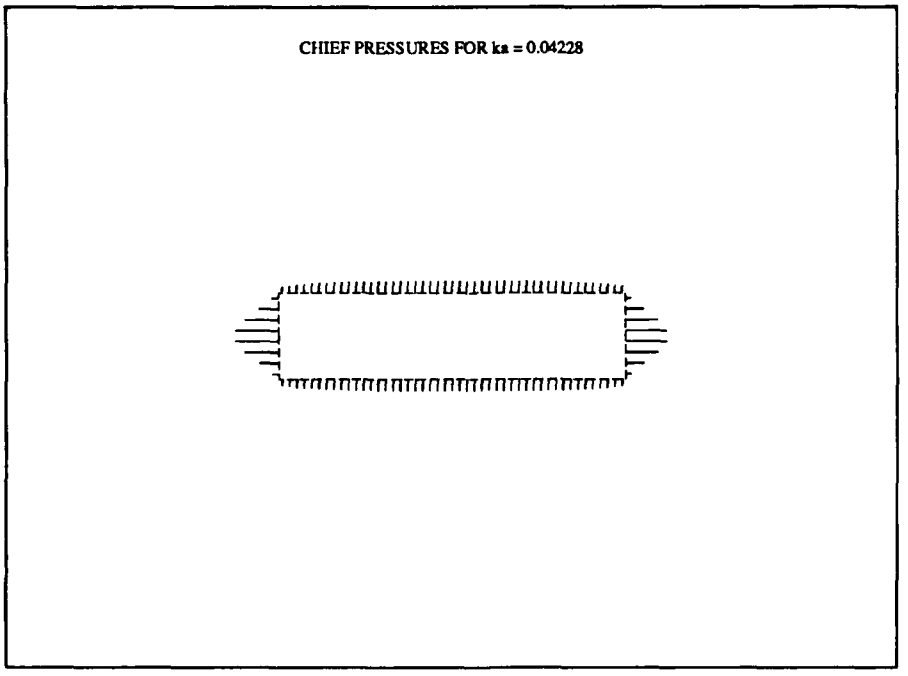

Figure 18. Surface pressure on cylinder, ka=0.04228.

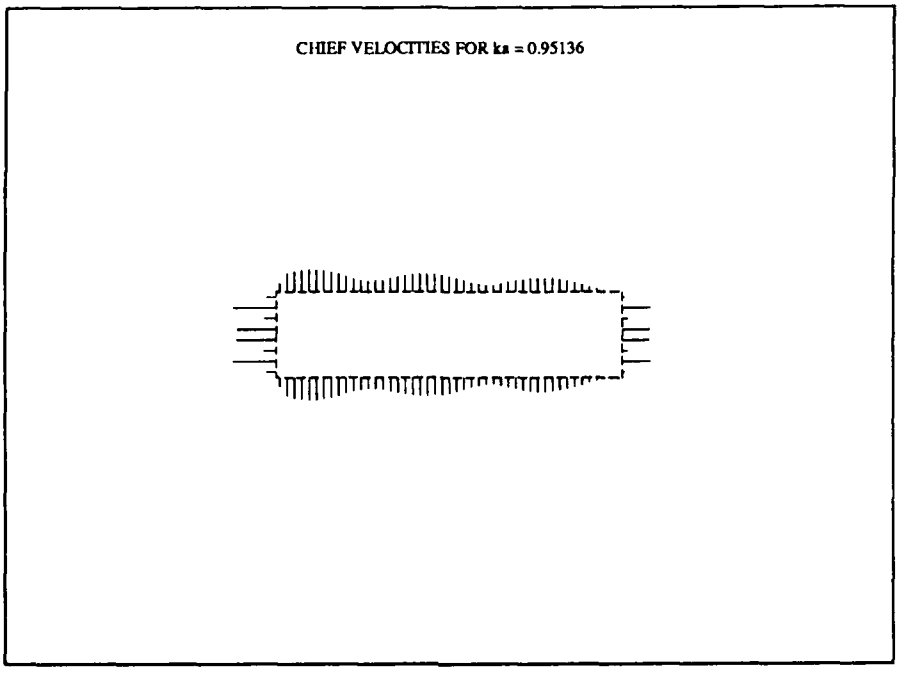

Figure 19. Normal velocity on cylinder, ka = 0.95136.

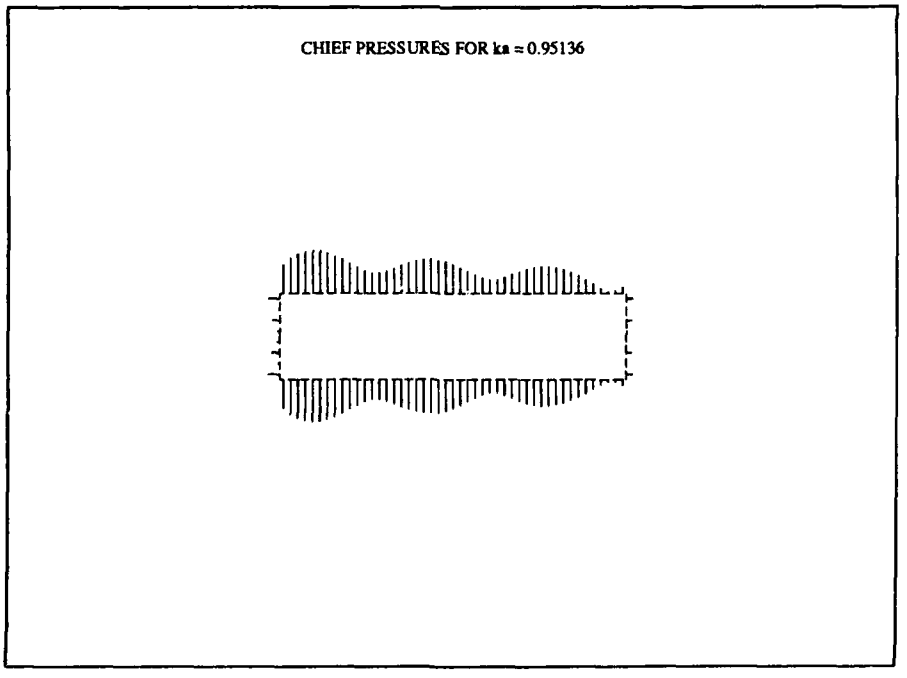

Figure 20. Surface pressure on cylinder ka = 0.95136.

Table 1. Sample modal identification scan.

ka	Mode #	Mag (dB)
0.025	2	27.1
0.050	2	32.2
	3	12.5
0.075	2	28.1
0.100	2	26.5
0.125	1	13.3
	2	25.3
	3	12.6
0.150	1	17.2
	2	24.3
	3	15.1
	4	10.5
0.175	1	21.0
	2	23.7
	3	17.5
	4	15.4
	5	10.4
0.200	1	26.2
	2	25.7
	3	20.4
	4	24.3
	5	20.1
0.225	1	46.1
	2	11.9
	3	33.0
	4	23.1
	5	45.7
	5	4.5
0.250	1	16.5
	3	15.4
	4	11.9
	5	25.4
0.275	3	18.5
	5	21.5
0.300	1	14.9
	3	19.6
	5	19.8

CONCLUSIONS

The scattering from elastic bodies immersed in a fluid is highly variable with frequency, due to the many resonant modes of the structure. Computational models for solving structural-acoustic scattering problems have been developed at NOSC. The scattered pressure field in these models can be represented as a sum of contributions from *in vacuo* modes of the structure. Although the overall spectral response of a scatterer is typically due to the contribution of hundreds of such modes, it has been shown that the response in narrow frequency bands (especially near sharp peaks) is often dominated by the contributions of a small number of modes. Auxiliary programs have been developed to identify and display these modal contributions along with the associated surface pressure and velocity distributions. The results obtained have provided valuable insight into the mechanisms responsible for features observed in the farfield response.

REFERENCES

Benthien, G., D. Barach, and D. Gillette. 1988. *CHIEF Users Manual*, NOSC Technical Document 970, revision 1.

Schenck, H.A. 1968. "Improved Integral Formulation for Acoustic Radiation Problems". *J. Acoust. Soc. Am.* 44:41–58.

Schenck, H.A., and G.W. Benthien. 1989. *Numerical Solution of Acoustic-Structure Interaction Problems*, NOSC Technical Report 1263.

Zienkiewicz, O.C. 1977. *The Finite Element Method*, Third Edition, McGraw-Hill, chapter 3.

INITIAL DISTRIBUTION

Naval Research Laboratory
Washington, DC 20375-5000
Dr. J. Bucaro
Dr. L. Dragonette
L. Shuetz

Naval Research Laboratory
Underwater Sound Reference Detachment
Orlando, FL 32856
Code 5970 (R. Timme)
Code 5976 (C. Siders)
Code 5976 (R. Montgomery)

David Taylor Research Center
Bethesda, MD 20084-5000
Dr. Y.N. Liu
M. Rummerman

Naval Underwater Systems Center
New London Laboratory
New London, CT 06320-5594
Code 2131 (J. Blottman)
Code 2132 (K. Webman)
Code 3234 (J. Lindberg)
Code 3322 (D. Bostian)
R. Radlinski
A. Carlson

Naval Sea Systems Command
Washington, DC 20362-5105
Code 55N2 (Dr. P.N. Majumdar)

Naval Surface Warfare Center Detachment
White Oak Laboratory
Silver Springs, MD 20903-5000
Dr. G. Gaunnard

Office of Naval Research
Arlington, VA 22217-5000
Code 1111 (John Lavery)

Naval Postgraduate School
Monterey, CA 93943
Prof. O.B. Wilson
Prof. Steve Baker

Catholic University of America
Washington, DC 20017
Prof. H. Uberall

University of Delaware
Newark, DE 19716
Prof. Robert P. Gilbert
Prof. George C. Hsiao
Prof. Ralph E. Kleinman

University of Colorado
Boulder, CO 80309-0449
Prof. Subhendu K. Datta

Georgia Institute of Technology
Atlanta, GA 30332
Prof. Jerry H. Ginsberg

Eastern Michigan University
Ypsilanti, MI 48197
James C. Porter

University of Kentucky
College of Engineering
Lexington, KY 40506-0046
Prof. A.F. Seybert

University of Texas at Austin
Austin, TX 78713-8029
Deborah A. Summa
Dr. Clark Penrod

University of Washington
Seattle, WA 98105
H.G. McMichael
N. Walden Barcus

Wayne State University
Detroit, MI 48202
Prof. X.F. Wu

AT&T Bell Laboratories
Whippany Road
Whippany, NJ 07981
Frank M. Labianca
Dr. David S. Burnett

INITIAL DISTRIBUTION (Continued)

Bendix Corporation
Oceanics Division
15825 Roxford Street
Sylmar, CA 91342-3597
Scott A. Hudson

Boeing Commercial Aircraft Company
A Division of the Boeing Company
P.O. Box 3707
Seattle, WA 98124-2207
Dr. G. Sengupta

Bolt, Baranek & Newman, Inc.
4015 Hancock Street, Suite 101
San Diego, CA 92110
Dr. Joel Young

General Electric Company
P.O. Box 4840
Syracuse, NY 13221
Michael H. Trent FRPI-A6
Leonard Longo EP5-F2

Global Associates, LTD
Engineering & Management Services
Number 4 Station Square
1423 Powhatan Street
Alexandria, VA 22314
Michael E. Buckman

Gould, Inc.
Ocean Systems Division
18901 Euclid Avenue
Cleveland, OH 44117
Stephen E. Hess

Hazeltine Corporation
115 Bay State Drive
Braintree, MA 02184
R. Grimes-Graeme

Honeywell, Inc.
6500 Harbour Heights Parkway
Everett, WA 98204-8899
Dr. Manuel Gonzales
Murray Simon

Hydroacoustics, Inc.
999 Lehigh Station Road
P.O. Box 23447
Rochester, NY 14692
Dr. R.F. Delacroix
Dr. J.V. Bouyoucos

Image Acoustics, Inc.
P.O. Box 6
N. Marshfield, MA 02059
Dr. John L. Butler

Rockwell International
3370 Mira Loma Avenue
P.O. Box 4921
Anaheim, CA 92803-4921
Charles P. Frahm

Sanders Associates, Inc.
H.W. Pope Technical Park #1
65 River Road, CS 907
Hudson, NH 03051-0907
Peter Harvey

Schlumberger
Old Quarry Road
Ridgefield, CT 06887-4108
Sergio Kostek

Science Applications International Corp.
803 West Broad Street, Suite 300
Falls Church, VA 22046
Georgio Borgiotti

SRI International
333 Ravenswood Avenue
Menlo Park, CA 94025
D. Kent Peterson

Texas Research Institute
9063 Bee Caves Road
Austin, TX 78733
L. Smith

Westinghouse Electric Corporation
P.O. Box 1488, MS 9845
Annapolis, MD 21404
L. Rowe

REPORT DOCUMENTATION PAGE

Form Approved
OMB No. 0704-0188

1. AGENCY USE ONLY *(Leave blank)*	2. REPORT DATE	3. REPORT TYPE AND DATES COVERED
	November 1989	Final

4. TITLE AND SUBTITLE
CONTRIBUTIONS OF INDIVIDUAL STRUCTURAL MODES TO THE SCATTERED ACOUSTIC FIELD

5. FUNDING NUMBERS
PE: 0602314N
RJ14B53
WU: DN308107

6. AUTHOR(S)
G. W. Benthien

7. PERFORMING ORGANIZATION NAME(S) AND ADDRESS(ES)
Naval Ocean Systems Center
San Diego, CA 92152-5000

8. PERFORMING ORGANIZATION REPORT NUMBER
NOSC TR 1329

9. SPONSORING/MONITORING AGENCY NAME(S) AND ADDRESS(ES)
Naval Research Laboratory
Washington, DC 20375-5000

10. SPONSORING/MONITORING AGENCY REPORT NUMBER

11. SUPPLEMENTARY NOTES

12a. DISTRIBUTION/AVAILABILITY STATEMENT
Approved for public release; distribution is unlimited.

12b. DISTRIBUTION CODE

13. ABSTRACT *(Maximum 200 words)*

The frequency behavior of the scattered acoustic field produced by a plane wave impinging on an elastic body immersed in an infinite fluid medium is dominated in certain frequency ranges by large peaks arising from resonant modes in the elastic structure. Computational models have been developed at the Naval Ocean Systems Center for solving these elastic scattering problems. This report shows that the scattered pressure can be represented as a sum of contributions from *in vacuo* modes of the structure. The spectral response of individual terms in this summation can be used to identify which modes contribute to each peak in the overall spectral response of the scattered field. In many cases a small number of modes dominate the response in the vicinity of these peaks.

14. SUBJECT TERMS
in vacuo modes
acoustics
acoustic scattering
vibration of structures
target strength

15. NUMBER OF PAGES
29

16. PRICE CODE

17. SECURITY CLASSIFICATION OF REPORT	18. SECURITY CLASSIFICATION OF THIS PAGE	19. SECURITY CLASSIFICATION OF ABSTRACT	20. LIMITATION OF ABSTRACT
UNCLASSIFIED	UNCLASSIFIED	UNCLASSIFIED	UNLIMITED